Biophysical Journal, Volume *116*

Supplemental Information

Understanding the Fluorescence Change in Red Genetically Encoded Calcium Ion Indicators

Rosana S. Molina, Yong Qian, Jiahui Wu, Yi Shen, Robert E. Campbell, Mikhail Drobizhev, and Thomas E. Hughes

Understanding the Fluorescence Change in Red Genetically Encoded Calcium Ion Indicators

Supporting Information

R.S. Molina[1], Y. Qian[2], J. Wu[2,3], Y. Shen[2], R.E. Campbell[2,4], M. Drobizhev[1], T.E. Hughes[1]

1. Department of Cell Biology & Neuroscience, Montana State University, Bozeman, Montana, USA
2. Department of Chemistry, University of Alberta, Edmonton, AB, Canada
3. Department of Pharmacology, Weill Cornell Medicine, New York, NY, USA
4. Department of Chemistry, The University of Tokyo, Tokyo, Japan

Supporting Materials and Methods

Protein purification

REX-GECO1 and jRGECO1a were cloned into the pUE backbone via ligation-independent cloning (In-Fusion, Clontech, Mountain View, CA). CAR-GECO1, K-GECO1, R-GECO1, R-GECO1.2, jRCaMP1a, and O-GECO1 were cloned into the pBAD backbone (Thermo Fisher Scientific, Waltham, MA) with restriction cloning. jREX-GECO1 was cloned into the modified pBAD backbone pTorPE with restriction cloning. All plasmids are available in Addgene. Plasmids were transformed into DH10B *E. coli*, which were grown for protein expression at 30°C for 2 days in Terrific Broth (BD, Sparks, MD) or Circlegrow (MP Biomedicals, Santa Ana, CA). To induce protein expression in the pBAD plasmids, 0.1% arabinose was added after growing approximately 5 hours. Bacteria pellets were lysed with BugBuster (EMD Millipore Corp., Burlington, MA) and the lysate was purified with His60 Ni Superflow Resin (Takara Bio, Mountain View, CA). Proteins were buffer-exchanged into pH 7.2 buffers containing 30 mM MOPS, 100 mM KCl, and 10 mM EGTA with or without 10 mM $CaCl_2$. Protein characterization was done in these respective buffers, except where noted. Purified proteins were stored short term ($\leq$ 2 weeks) at 4°C and long term at -80°C. The Ca^{2+}-free form of K-GECO1 exhibits photoswitching in room light; so the protein sample was stored covered in foil, and all of the photophysical measurements were done with minimal exposure to room light.

Special corrections for pH titrations

For the titrations of the Ca^{2+}-saturated state of jREX-GECO1 and REX-GECO1 from pH 7.2 and higher, the OD at the peak of the anionic form absorbance was corrected for the absorbance of the neutral form at that position (Eq. S1):

$$OD_A^A = \frac{OD_{A+N}^A - OD_{A+N}^N \cdot (OD_N^A / OD_N^N)}{1 - (OD_N^A / OD_N^N) \cdot (OD_A^N / OD_A^A)} \quad \text{(S1)}$$

Here, the superscript indicates the spectral position of the OD value, either at the anionic peak position (^{A}) or the neutral peak position (^{N}). The subscript indicates the form of the chromophore that the OD belongs to, either anionic and neutral ($_{A+N}$), only anionic ($_A$), or only neutral ($_N$). The fractions (OD_N^A / OD_N^N) and (OD_A^N / OD_A^A) were considered constant throughout the titration. The former was determined based on the spectrum at pH 7.2 (assuming 100% neutral form), and the latter was based on the spectrum at the pH where the anionic form reached its maximum.

Special corrections for determination of the relative fraction of the excitable form of the chromophore

In the case of K-GECO1 and CAR-GECO1, the absorbance at pH 7.2 include significant absorption from other, non-red chromophore(s) which overlap with the absorption of the neutral form of the red chromophore. Their absorbance spectra were unmixed using excitation spectra in order to find the peak OD of the red neutral chromophore (Fig. S13).

For both the Ca^{2+}-free and Ca^{2+}-saturated spectra of K-GECO1, the red anionic form excitation spectrum (shifted to match the peak position if necessary) was fitted to the absorbance spectrum and subtracted, leaving only the absorption of the neutral chromophore and the unknown form (peaking near 400 nm). To this we fit the red neutral form excitation spectrum and took the peak value as the OD of the neutral chromophore (Fig. S13A and B). The anionic form excitation spectrum was measured with the Ca^{2+}-saturated sample with emission registration at 700 nm. The neutral form excitation spectrum was measured with the Ca^{2+}-free sample with emission registration at 530 nm.

For the Ca^{2+}-saturated state of CAR-GECO1, the excitation spectrum of the immature anionic green chromophore was subtracted from the absorbance spectrum and then the red neutral form excitation spectrum was fitted under the difference spectrum to find the OD (Fig. S13C). For the Ca^{2+}-free state, the red neutral form excitation spectrum was fitted to the unadulterated spectrum (Fig. S13D). The anionic green chromophore excitation spectrum was measured from Ca^{2+}-saturated CAR-GECO1 with emission registration at 540 nm. The red neutral form excitation spectrum was measured scanning the Ca^{2+}-free sample with emission registration at 540 nm.

Emission spectra

The LS 55 Fluorescence Spectrometer (PerkinElmer, Waltham, MA) was used to collect emission spectra with 10 nm excitation slits and 5 nm emission slits. The emission spectra were corrected for spectral sensitivity of the detection system by applying a correction function created with the Spectral Fluorescence Standard Kit (Millipore-Sigma, Darmstadt, Germany).

Structural analysis

The illustration of the K-GECO1 crystal structure in Fig. 2A and structural analyses from the discussion were performed with the UCSF Chimera package (University of California, San Francisco, CA). Chimera is developed by the UCSF Resource for Biocomputing, Visualization, and Informatics (supported by NIGMS P41-GM103311).

Development and Ca^{2+} K_d determination of jREX-GECO1

To increase the Ca^{2+} affinity of REX-GECO1 (1), the Q306D and M339F mutations were introduced using the QuikChange Mutagenesis Kit (Agilent Technologies, Santa Clara, CA). These two mutations were reported to be responsible for the increased Ca^{2+} affinity of jRGECO1a (2) relative to R-GECO1. The resulting variant was designated as jREX-GECO1. To determine the K_d of jREX-GECO1, Ca^{2+} titrations were performed using EGTA-buffered Ca^{2+} solutions as previously described (3). Briefly, purified proteins were diluted into a series of buffers with free Ca^{2+} concentrations ranging from 0 nM to 39 μM at 25 °C. These buffered Ca^{2+} solutions were prepared by mixing a CaEGTA buffer (30 mM MOPS, 100 mM KCl, 10 mM EGTA, 10 mM $CaCl_2$) and an EGTA buffer (30 mM MOPS, 100 mM KCl, 10 mM EGTA) at appropriate ratios. Fluorescence intensities were measured and plotted against Ca^{2+} concentrations and fitted by a sigmoidal binding function to extract the Hill coefficient and K_d for Ca^{2+}.

Table S1. Additional biophysical properties of the red GECIs.

Class	Protein	Ca^{2+}	pK_a(s), this work	pK_a, literature	K_d for Ca^{2+} (nM)	Hill Coefficient	λ_{Rmax} (nm)	$\varepsilon_e(\lambda_{Rmax})$ ± 5% ($mM^{-1}cm^{-1}$)	$\sigma_{2,e}$ (λ_{Rmax}) ± 17% (GM)	$F_1(\lambda_{Rmax})$ ± 13% ($mM^{-1}cm^{-1}$)	$F_2(\lambda_{Rmax})$ ± 21% (GM)
I	R-GECO1	-	8.69 ± 0.03	8.9[a], 8.7[b]	482[a], 337[b], 449[c]	2.06[a], 2[b], 1.51[c]	516	27	16	0.23	0.14
		+	5.21 ± 0.02, 7.1 ± 0.1, 10.33 ± 0.05	6.59[a], 6.4[b]				32	26	5.3	4.4
	R-GECO1.2	-	8.98 ± 0.02	8.93[d]	1200[d]	2.79[d]	514	23	14	0.16	0.10
		+	5.42 ± 0.02, 8.0 ± 0.3, 10.77 ± 0.05	5.99[d]				30	28	7.3	7
	jRGECO1a	-	8.63 ± 0.03	8.6[b]	148[b]	1.9[b]	514	26	11	0.25	0.10
		+	4.97 ± 0.03, 6.74 ± 0.08, 10.51 ± 0.06	6.3[b]				33	26	5.9	5
	O-GECO1	-	9.52 ± 0.01	9.44[d]	1500[d]	2.06[d]	502	26	13	0.04	0.021
		+	6.24 ± 0.01, 11.25 ± 0.09	6.07[d]				29	20	5.9	4.2
	CAR-GECO1	-	8.96 ± 0.02	9.05[d]	490[d]	2.01[d]	516	31	16	0.20	0.10
		+	5.29 ± 0.01, 8.4 ± 0.2, 10.5 ± 0.1	5.74[d]				35	31	8.2	7
II	K-GECO1	-	6.71 ± 0.04, 8.23 ± 0.04		165[e]	1.12[e]	530	39	15	1.9	0.7
		+	6.34 ± 0.03					44	22	16	8
	jRCaMP1a	-	6.48 ± 0.05	5.6[b]	214[b]	0.86[b]	518	27	17	4.3	2.7
		+	6.20 ± 0.03	6.4[b]				26	16	11	7
III	REX-GECO1	-	4.6 ± 0.2, 7.6 ± 0.2, 10.0 ± 0.1	6.5[f]	240[f]	1.8[f]	450	7.0	8.2	0.16	0.19
		+	11.70 ± 0.02					25	33	5.2	7
	jREX-GECO1	-	4.6 ± 0.1, 7.80 ± 0.04, 9.67 ± 0.05		200	1.67	450	8.2	10	0.18	0.23
		+	11.63 ± 0.02					26	36	5.4	7

References:

[a] (3)

[b] (2)

[c] (4)

[d] (5)

[e] (6)

[f] (1)

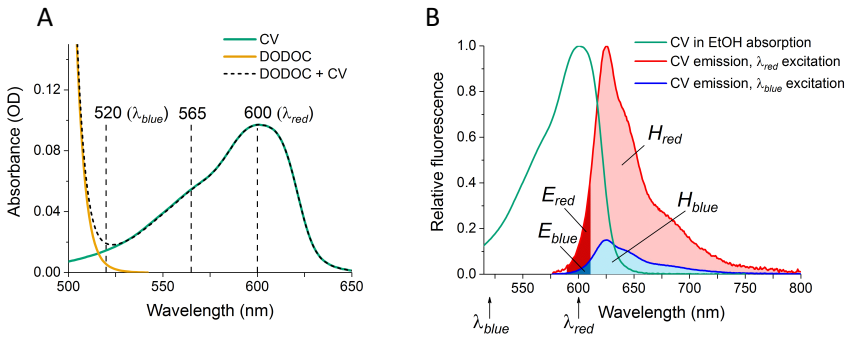

Figure S1. Analytical method to find correct fluorescence quantum yield, as described in Materials and Methods. Demonstrated in a mixture of 6.5 µM 3,3′-Dioctadecyloxacarbocyanine perchlorate (DODOC) and 1.2 µM Cresyl Violet (CV) in ethanol. (*A*) Absorbance spectrum of the mixture with respective spectra of CV and DODOC fitted underneath. Dashed lines indicate the excitation wavelengths used in the integrating sphere to get the quantum yield of CV. (*B*) Illustration of the "very short" (*E*) and "short" (*H*) fluorescence integrals for λ_{blue} and λ_{red} excitation of CV. The normalized absorption of CV is shown for reference. E_{blue} is shaded dark blue; E_{red} is dark red; H_{blue} is light blue; and H_{red} is pink.

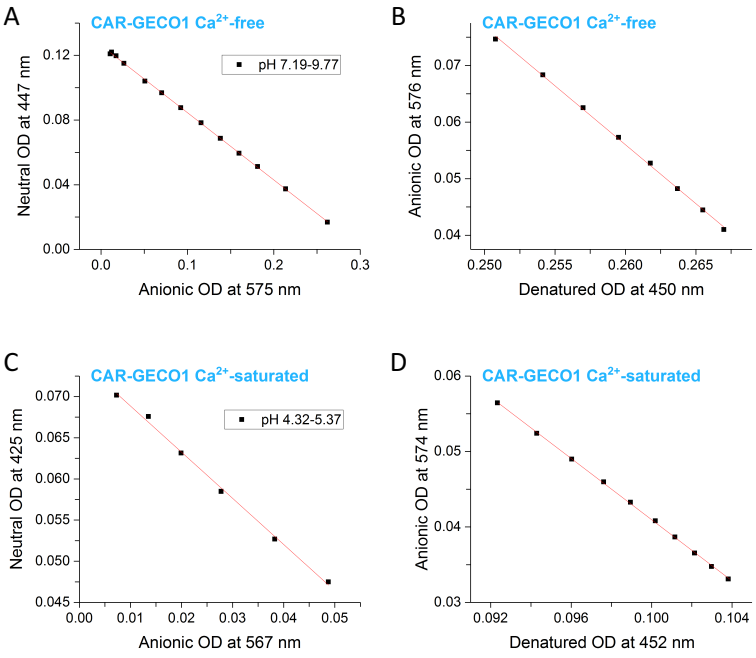

Figure S2. Example plots with fitted linear slope used to determine the neutral and anionic extinction coefficients for some of the red GECIs, as explained in Materials and Methods. Shown is data from the CAR-GECO1 pH titrations.

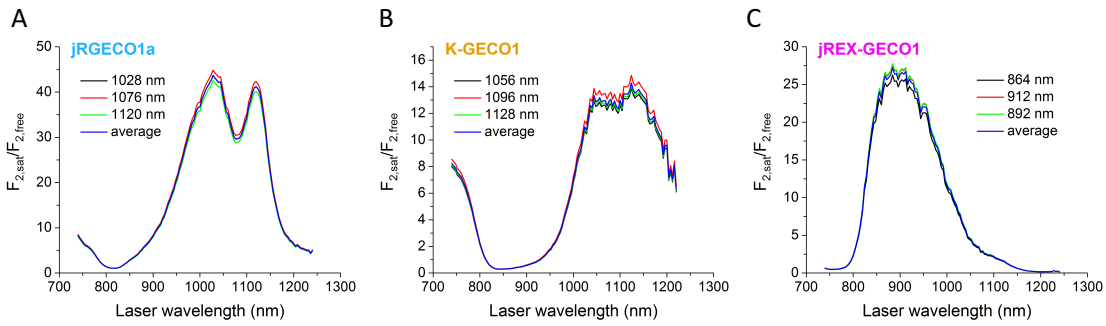

Figure S3. Normalizing the Ca^{2+}-saturated/free F_2 ratio spectra to the ratios determined at three excitation wavelengths around the maximum. Shown are the ratio spectra normalized to the three wavelengths separately and then averaged for jRGECO1a, K-GECO1, and jREX-GECO1 as examples.

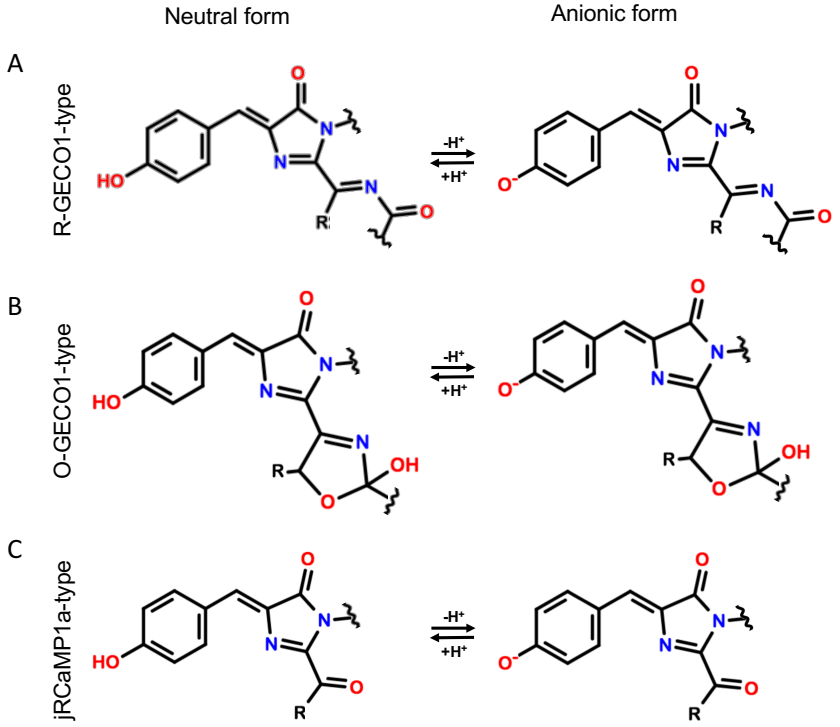

Figure S4. Illustration of the neutral and anionic forms of the chromophores in the red GECIs under study. (*A*) R-GECO1-type chromophore, same as Fig. 2D in main text (PDB ID: 4I2Y (4)). (*B*) O-GECO1-type chromophore (from mOrange structure, PDB ID: 2H5O (7)). (*C*) jRCaMP1a-type chromophore (from RCaMP structure, PDB ID: 3U0K (4)).

1. R-GECO1
2. R-GECO1.2
3. jRGECO1a
4. O-GECO1
5. CAR-GECO1
6. REX-GECO1
7. jREX-GECO1
8. jRCaMP1a
9. K-GECO1

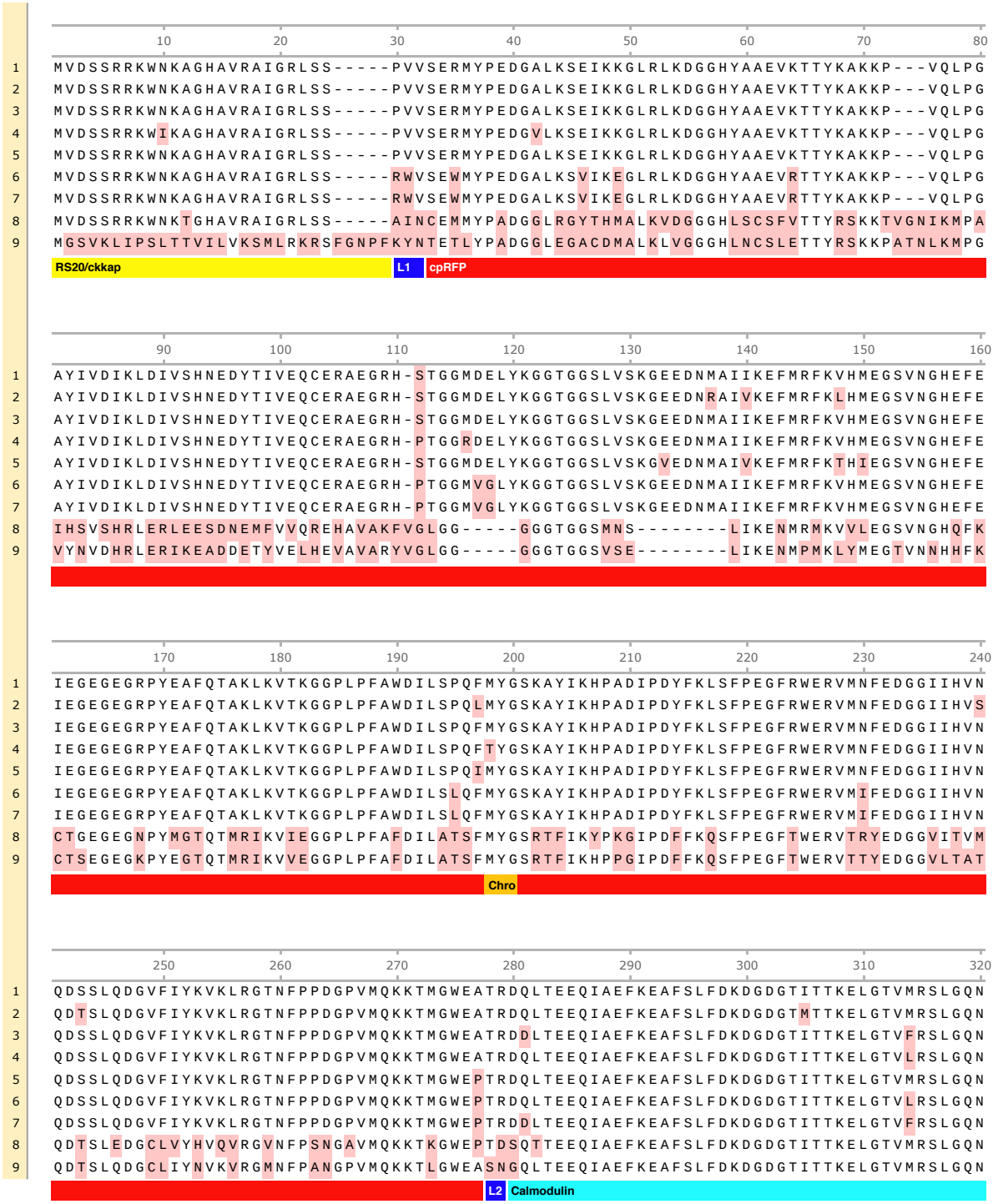

Figure S5 (*continued on next page with legend*). Protein sequence alignment of red GECIs under study.

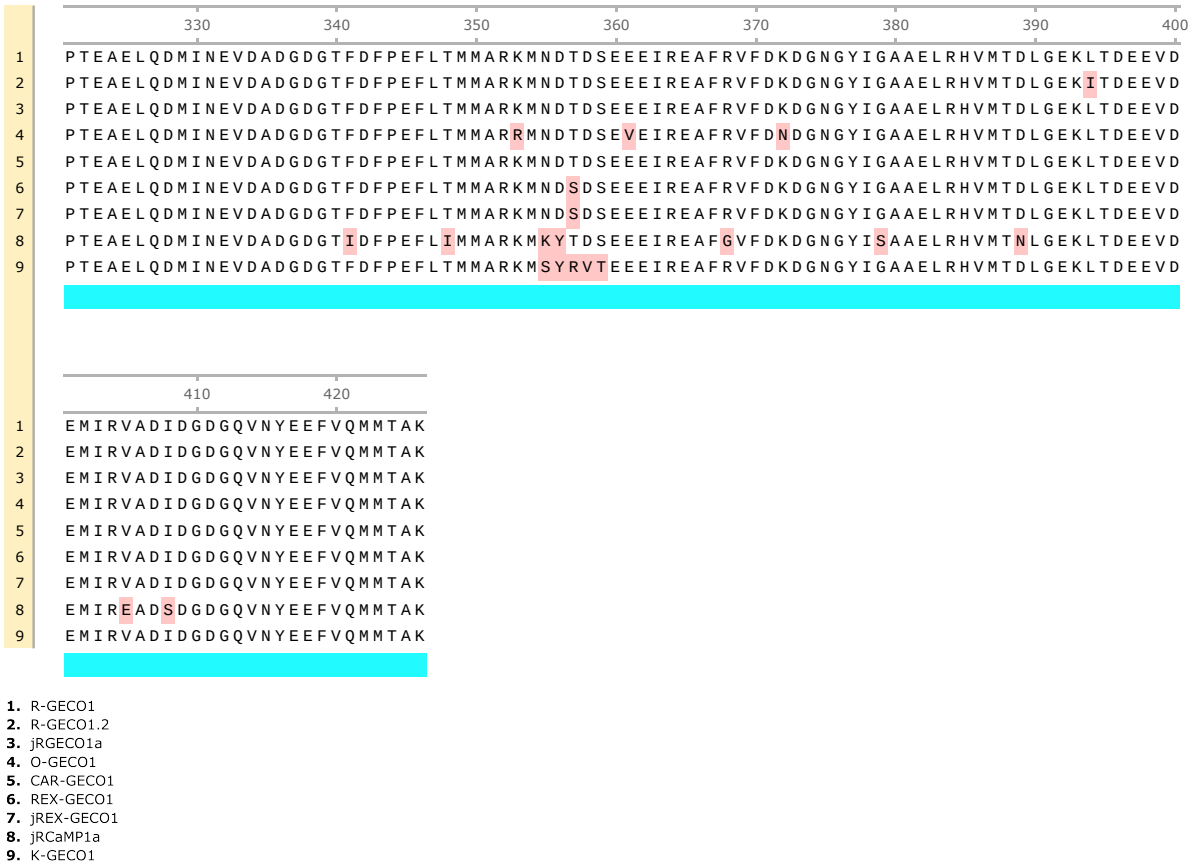

Figure S5 (*continued from previous page*). Protein sequence alignment of red GECIs under study. Residues that differ from the consensus sequence are highlighted in pink. The colored bars underneath the sequence indicate the respective parts of the protein: the CaM-binding peptide RS20 or ckkap is yellow; linkers 1 and 2 are blue; the circularly-permuted red FP is red with the chromophore sequence in gold; and calmodulin is aqua.

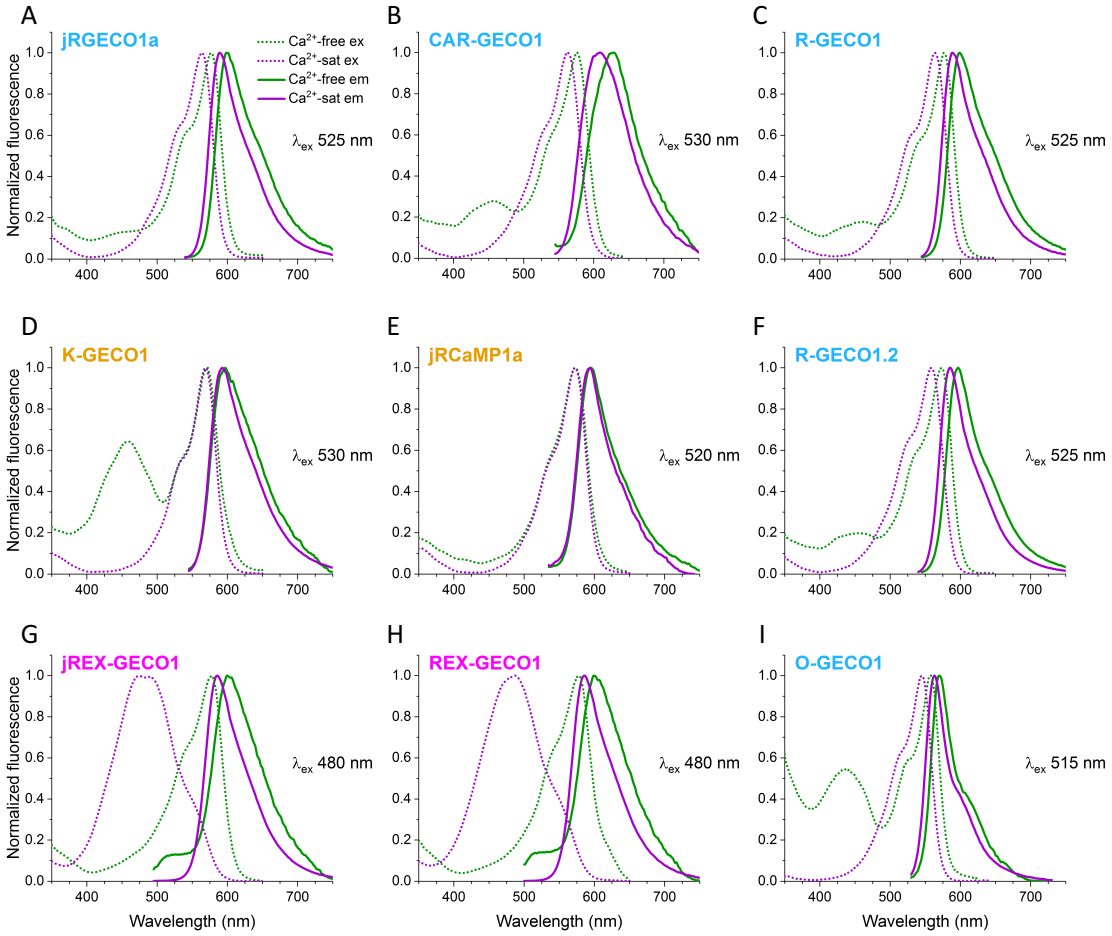

Figure S6. Excitation (one-photon) spectra (ex) and emission spectra (em) of the Ca^{2+}-free and Ca^{2+}-saturated states for each protein. All spectra are normalized to 1. The excitation spectra were scanned while collecting the entire integrated fluorescence spectrum by setting the emission grating to the 0-th diffraction order. The excitation wavelength of light used when scanning the emission spectrum is indicated on each plot.

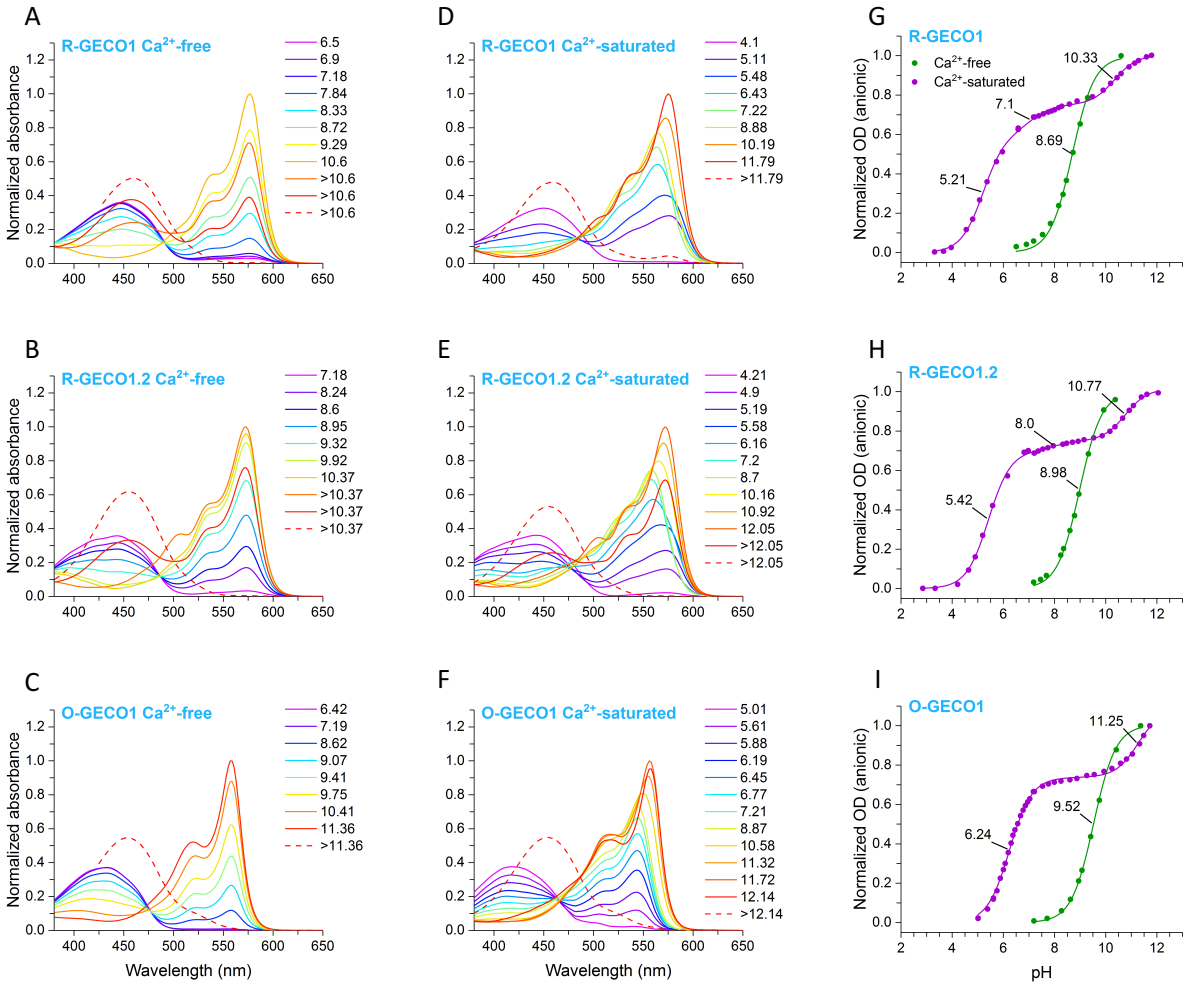

Figure S7. Plotted as in Fig. 4 of the main text and Fig. S8. Titrations from neutral to acidic pH and neutral to alkaline pH were done separately and then combined. The figures are normalized to the observed maximal absorbance of the anionic form. (*A-F*) Absorbance pH titrations, measured in either Ca^{2+}-free or Ca^{2+}-saturated buffer as noted. Each spectrum was measured at the pH value designated in the legends. The final spectrum (red dashed line) belongs to the denatured chromophore. (*G-I*) Apparent pK_a curves, showing the OD of the anionic form as a function of pH. The pK_a values are indicated on the fitted curve.

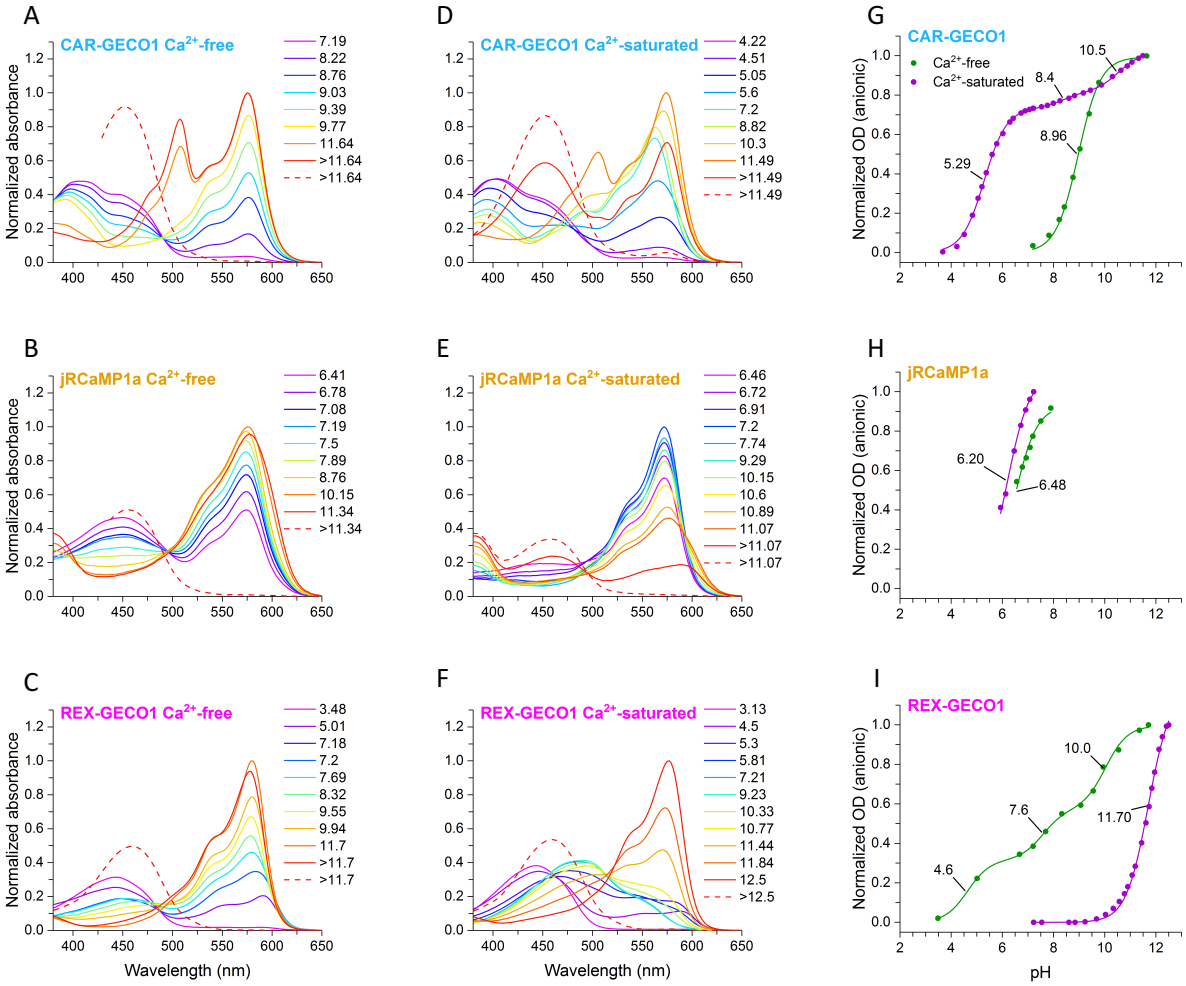

Figure S8. Plotted as in Fig. 4 of the main text and Fig. S7. Titrations from neutral to acidic pH and neutral to alkaline pH were done separately and then combined. The figures are normalized to the observed maximal absorbance of the anionic form. (*A-F*) Absorbance pH titrations, measured in either Ca^{2+}-free or Ca^{2+}-saturated buffer as noted. Each spectrum was measured at the pH value designated in the legends. The final spectrum (red dashed line) belongs to the denatured chromophore. (*G-I*) Apparent pK_a curves, showing the OD of the anionic form as a function of pH. The pK_a values are indicated on the fitted curve. (*H*) Only part of the jRCaMP1a titrations could be fitted because of protein precipitation at pH values below those displayed and early denaturation of the anionic form at higher pH values.

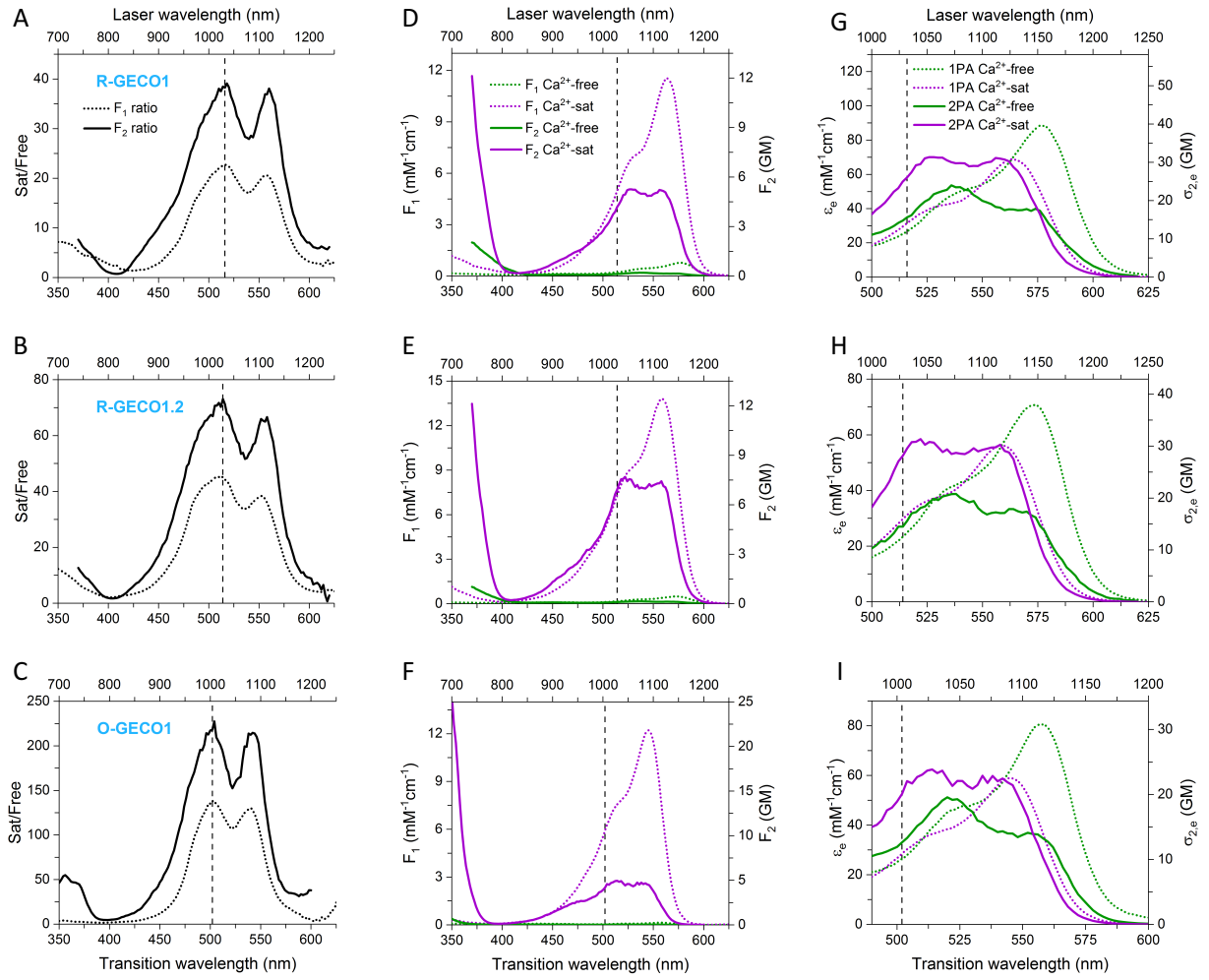

Figure S9. Spectral analysis of R-GECO1 (row 1), R-GECO1.2 (row 2), and O-GECO1 (row 3). Plots are set up as in Fig. 5 of main text and Fig. S10. The vertical dashed line on each plot indicates the transition wavelength of excitation (λ_{Rmax}) where the Ca^{2+}-saturated/free F_1 and F_2 ratios are approximately maximum. (*A-C*) Ca^{2+}-saturated/free (Sat/Free) F_1 (dotted line) and F_2 (solid line) ratios as a function of excitation wavelength, measured directly by taking the ratio of the integrated fluorescence signal normalized to the known relative protein concentration between the Ca^{2+}-free and Ca^{2+}-saturated samples. (*D-F*) Spectra of the one-photon brightness (F_1, dotted lines, left and bottom axes) and two-photon brightness (F_2, solid lines, right and top axes) of the Ca^{2+}-free and Ca^{2+}-saturated states. (*G-I*) One-photon absorption (1PA) and two-photon absorption (2PA) of the excitable form of the chromophore, shown in values of ε_e (left and bottom axes) and $\sigma_{2,e}$ (right and top axes), respectively, for the Ca^{2+}-free and Ca^{2+}-saturated states.

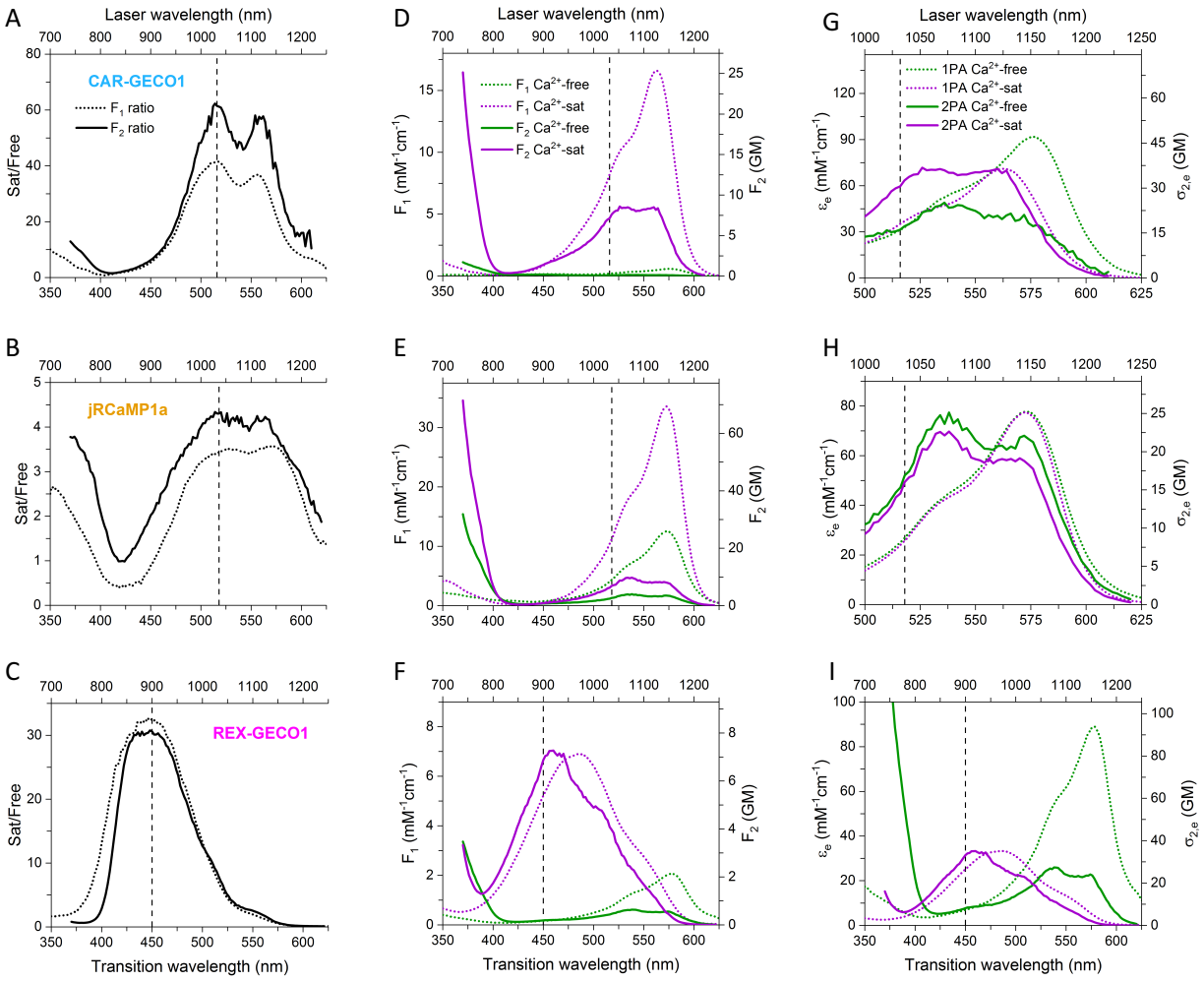

Figure S10. Spectral analysis of CAR-GECO1 (row 1), jRCaMP1a (row 2), and REX-GECO1 (row 3). Plots are set up as in Figure 5 of main text and Figure S9. The vertical dashed line on each plot indicates the transition wavelength of excitation (λ_{Rmax}) where the Ca^{2+}-saturated/free F_1 and F_2 ratios are approximately maximum. (*A-C*) Ca^{2+}-saturated/free (Sat/Free) F_1 (dotted line) and F_2 (solid line) ratios as a function of excitation wavelength, measured directly by taking the ratio of the integrated fluorescence signal normalized to the known relative protein concentration between the Ca^{2+}-free and Ca^{2+}-saturated samples. (*D-F*) Spectra of the one-photon brightness (F_1, dotted lines, left and bottom axes) and two-photon brightness (F_2, solid lines, right and top axes) of the Ca^{2+}-free and Ca^{2+}-saturated states. (*G-I*) One-photon absorption (1PA) and two-photon absorption (2PA) of the excitable form of the chromophore, shown in values of ε_e (left and bottom axes) and $\sigma_{2,e}$ (right and top axes), respectively, for the Ca^{2+}-free and Ca^{2+}-saturated states.

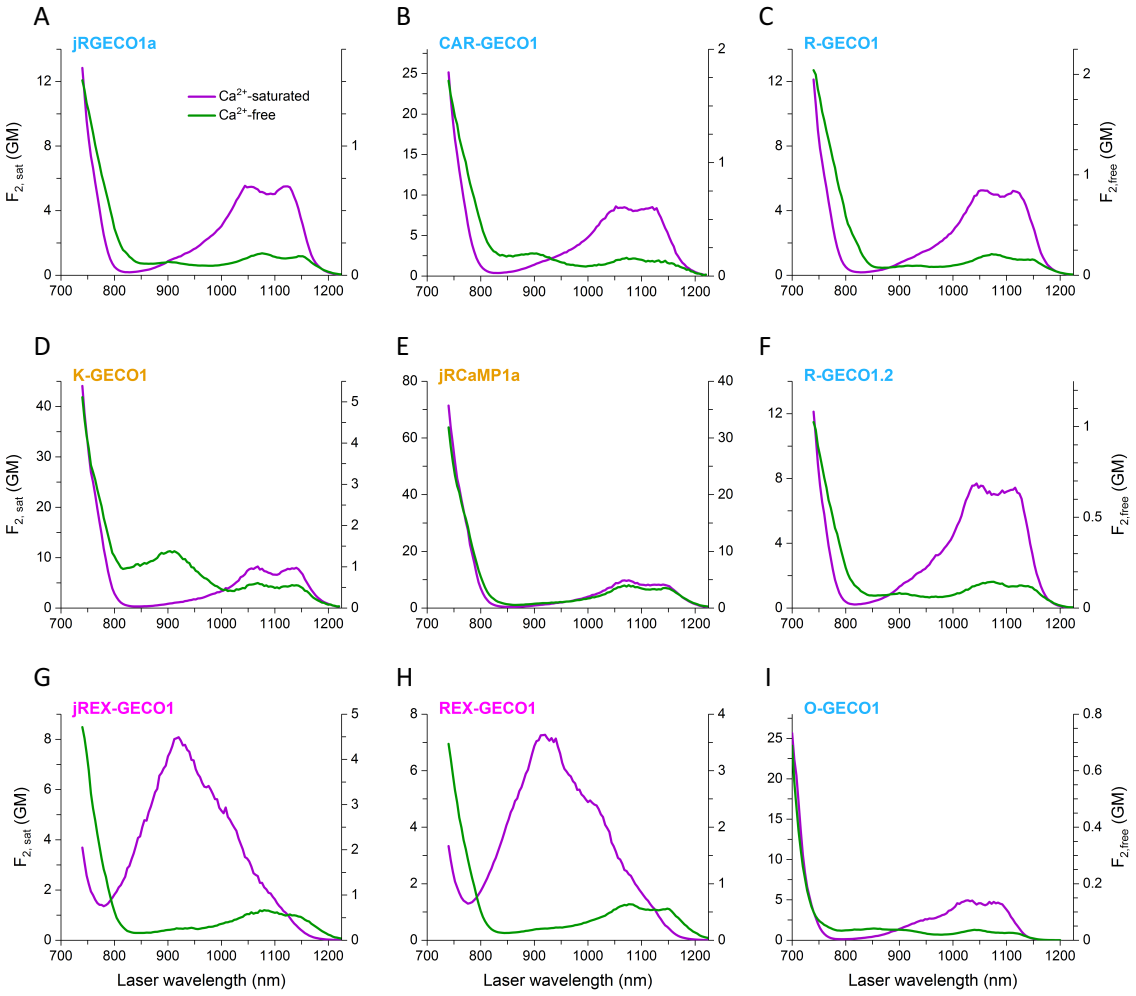

Figure S11. Two-photon absorption spectra plotted according to two-photon brightness. The scale for the Ca^{2+}-saturated spectra is on the left, and the scale for the Ca^{2+}-free spectra is on the right.

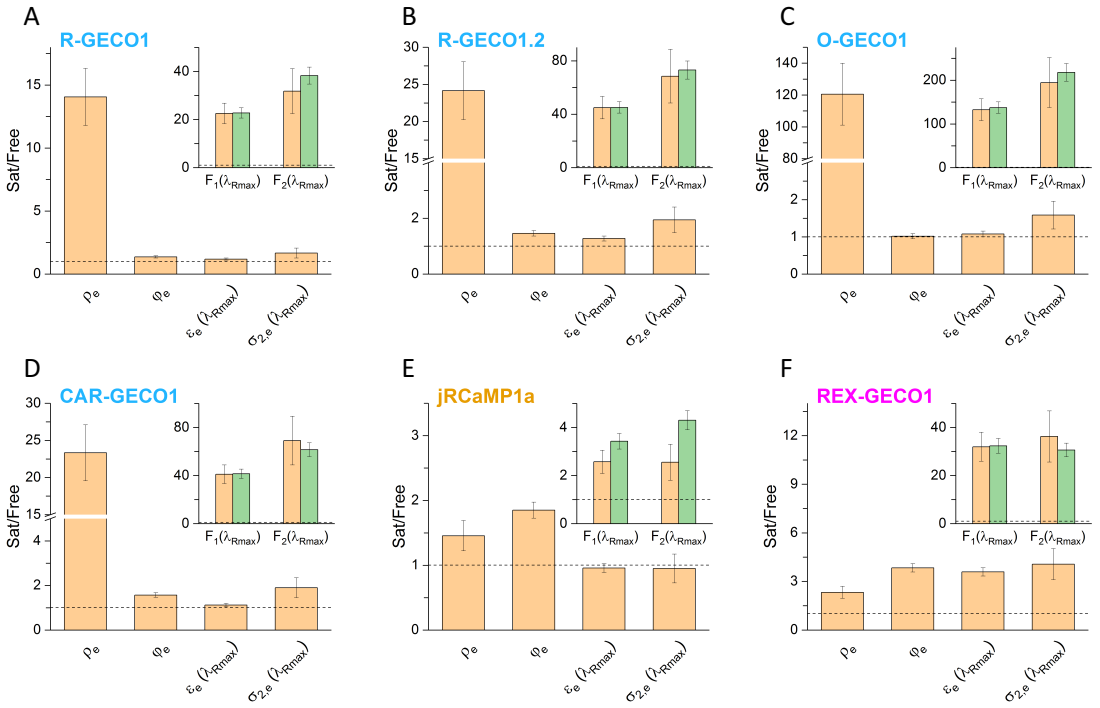

Figure S12. Plotted as in Fig. 6 of main text. Ca^{2+}-saturated/free ratios (Sat/Free) for ρ_e, φ_e, $\varepsilon_e(\lambda_{Rmax})$, and $\sigma_{2,e}(\lambda_{Rmax})$. Insets: Ca^{2+}-saturated/free F_1 and F_2 ratios, both calculated from the independent measurements of ρ_e, φ_e, ε_e, and $\sigma_{2,e}$ (tan) and measured directly (green) as described in Fig. 5 of main text. The horizontal dashed line marks a Sat/Free ratio of 1 (no change) for each plot. Error bars represent estimated standard deviations.

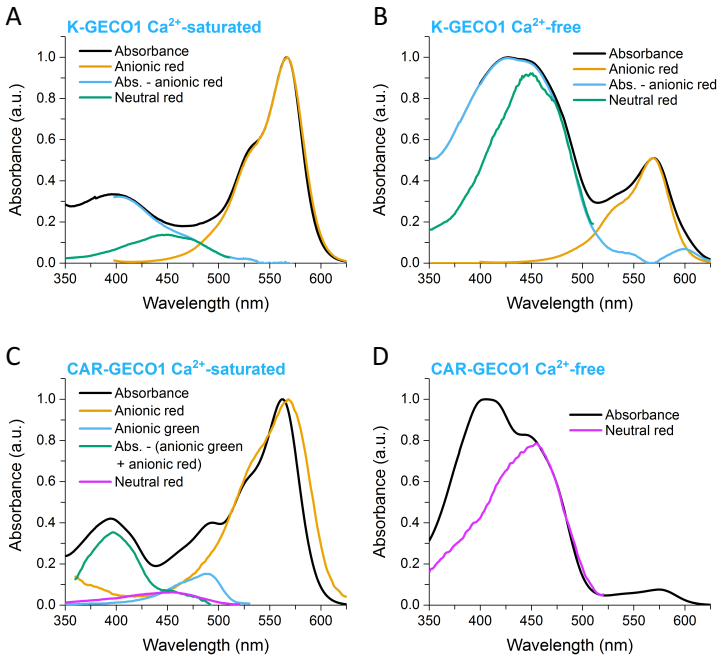

Figure S13. Separating the components of the absorbance spectra of K-GECO1 and CAR-GECO1 using excitation spectra as described in Supporting Materials and Methods.

Supporting References

1. Wu, J., A.S. Abdelfattah, L.S. Miraucourt, E. Kutsarova, A. Ruangkittisakul, H. Zhou, K. Ballanyi, G. Wicks, M. Drobizhev, A. Rebane, E.S. Ruthazer, and R.E. Campbell. 2014. A long Stokes shift red fluorescent Ca^{2+} indicator protein for two-photon and ratiometric imaging. Nat. Commun. 5: 5262.

2. Dana, H., B. Mohar, Y. Sun, S. Narayan, A. Gordus, J.P. Hasseman, G. Tsegaye, G.T. Holt, A. Hu, D. Walpita, R. Patel, J.J. Macklin, C.I. Bargmann, M.B. Ahrens, E.R. Schreiter, V. Jayaraman, L.L. Looger, K. Svoboda, and D.S. Kim. 2016. Sensitive red protein calcium indicators for imaging neural activity. Elife. 5.

3. Zhao, Y., S. Araki, J. Wu, T. Teramoto, Y.-F. Chang, M. Nakano, A.S. Abdelfattah, M. Fujiwara, T. Ishihara, T. Nagai, and R.E. Campbell. 2011. An expanded palette of genetically encoded Ca^{2+} indicators. Science. 333: 1888–1891.

4. Akerboom, J., N. Carreras Calderón, L. Tian, S. Wabnig, M. Prigge, J. Tolö, A. Gordus, M.B. Orger, K.E. Severi, J.J. Macklin, R. Patel, S.R. Pulver, T.J. Wardill, E. Fischer, C. Schüler, T.-W. Chen, K.S. Sarkisyan, J.S. Marvin, C.I. Bargmann, D.S. Kim, S. Kügler, L. Lagnado, P. Hegemann, A. Gottschalk, E.R. Schreiter, and L.L. Looger. 2013. Genetically encoded calcium indicators for multi-color neural activity imaging and combination with optogenetics. Front. Mol. Neurosci. 6: 2.

5. Wu, J., L. Liu, T. Matsuda, Y. Zhao, A. Rebane, M. Drobizhev, Y.-F. Chang, S. Araki, Y. Arai, K. March, T.E. Hughes, K. Sagou, T. Miyata, T. Nagai, W.-H. Li, and R.E. Campbell. 2013. Improved orange and red Ca^{2+} indicators and photophysical considerations for optogenetic applications. ACS Chem. Neurosci. 4: 963–972.

6. Shen, Y., H. Dana, A.S. Abdelfattah, R. Patel, J. Shea, R.S. Molina, B. Rawal, V. Rancic, Y.-F. Chang, L. Wu, Y. Chen, Y. Qian, M.D. Wiens, N. Hambleton, K. Ballanyi, T.E. Hughes, M. Drobizhev, D.S. Kim, M. Koyama, E.R. Schreiter, and R.E. Campbell. 2018. A genetically encoded Ca^{2+} indicator based on circularly permutated sea anemone red fluorescent protein eqFP578. BMC Biol. 16: 9.

7. Shu, X., N.C. Shaner, C.A. Yarbrough, R.Y. Tsien, and S.J. Remington. 2006. Novel chromophores and buried charges control color in mFruits. Biochemistry. 45: 9639–9647.